The sum of the terms with $l+m=3$ equals:

$$a_{k,1,2}+p\,a_{k-1,1,2}+a_{k,3,0}+3\,p\,a_{k-1,3,0} \qquad (14)$$
$$+3\,p^2\,a_{k-2,3,0}+p^3\,a_{k-3,3,0}=0\,.$$

From (7), it follows that:

$$(l+1)\,(l+2)\,a_{k,l+2,0}=(-1)^k\sum_{i=1}^{k+1}\{(-1)^i\,i\,a_{i,l,0}\} \qquad (15)$$
$$-(k+1)\,(k+2)\,a_{k+2,l,0}\,.$$

On expressing the coefficients with $l=3$ in (14) in coefficients with $l=1$ by means of (15), we arrive at the equality:

$$a_{k,1,2}+p\,a_{k-1,1,2}=(-1)^k\,\frac{p-p^2}{6} \qquad (16)$$

and because of (12):

$$a_{k,1,2}=(-1)^k\,\frac{p-p^{k+1}}{6}\,. \qquad (17)$$

The v-component of the field strength in the median plane may be found from (1), and a summation of (13) and (17):

$$B_v=B\left[\frac{1}{1+p\,u}+\frac{b^2}{6}\left\{\frac{p\,u}{1+u}-\frac{p^2\,u}{1+p\,u}\right\}+\dots\right]. \qquad (18)$$

The parameters used in the previous article [1] are related to the coefficients $a_{k,l}$ in (2) through:

$$a_{01}=-1\,; \qquad a_{11}=n\,; \qquad (19)$$
$$a_{21}=\tfrac{1}{2}\{X(1-n)-2\,n\}\,; \quad a_{31}=-C_3\,;\ a_{41}=-C_4\,.$$

By reversion of the series one finds the required cone angle for a prescribed n to be defined through:

$$p=n+\frac{1}{6}\,n(1-n)\,b^2+\dots, \qquad (20)$$

whereas the resulting field shape is represented by:

$$X=2\,n+\frac{1}{3}\,n(1-n)\,b^2+\dots,$$
$$C_3=-n^3+\frac{1}{6}\,n(1-n)^2\,(1+2\,n)\,b^2+\dots, \qquad (21)$$
$$C_4=n^4-\frac{1}{6}\,n(1-n)^2(1+2\,n+3\,n^2)b^2+\dots\,.$$

The omitted terms in (20) and (21) are of the order b^4.

The results of this work were obtained independently by the three authors by different methods. The derivation of one of us (A. J. H. B.) was presented in this paper.

The authors wish to thank Prof. Dr. J. KISTEMAKER and Prof. H. EWALD respectively for their stimulating interest.

The work made in Amsterdam is part of the program of research of the Stichting voor Fundamenteel Onderzoek der Materie and was made possible by financial support of the Nederlandse Organisatie voor Zuiver Wetenschappelijk Onderzoek. The work made in Munich was made possible by financial support of the Bundesministerium für Atomkernenergie und Wasserwirtschaft in Bad Godesberg.

Calculation of the Ion Optical Properties of Inhomogeneous Magnetic Sector Fields, Part 2: The Second Order Aberrations Outside the Median Plane

By H. WACHSMUTH,

Physikalisches Institut der Technischen Hochschule, München,

and A. J. H. BOERBOOM and H. A. TASMAN,

F.O.M.-Laboratorium voor Massaspectrografie, Amsterdam, Holland

(Z. Naturforschg. 14 a, 818—822 [1959]; eingegangen am 14. Juni 1959)

In a previous article [1] we pointed out the possible advantages of inhomogeneous magnetic sector fields for mass spectrometers, as these fields permit a substantial increase in mass dispersion and resolving power without change in radius or slit widths. In the said paper [1] we calculated the coefficients of the second order aberrations in the median plane, as well as the field shape required to eliminate the second order angular aberration in the median plane. In the present paper we calculate the second order aberrations outside the median plane referring to focusing in the radial direction. Again the influence of fringing fields is being neglected, and the field boundaries are supposed to be plane and normal to the main path at the point where it enters and leaves the field.

The use of an inhomogeneous magnetic analysing field for a mass spectrometer may result in a greatly enlarged mass dispersion and resolving power without change in radius or slit widths. We discussed

[1] H. A. TASMAN and A. J. H. BOERBOOM, Z. Naturforschg. **14 a**, 121 [1959].

this matter in a previous article, and calculated the second order approximation of the ion trajectories in the median plane and the first order approximation outside the medium plane (TASMAN and BOERBOOM [1]).

In the present paper we present the coefficients of the second order aberrations outside the median plane, but only for focusing in radial or y-direction. As these fields do not possess in general a stigmatic focusing property, no first order focusing in axial or z-direction is achieved, and hence the second order aberrations for z-focusing are irrelevant as they are small as compared with the first order aberrations.

Again the median plane is supposed to be a plane of symmetry. The relevant second order aberrations impairing y-focusing may be split up into six terms. Three of these exist in the median plane: the second order angular aberration $(:)\ \alpha^2$; the second order velocity aberration $(:)\ \beta^2$; and the mixed second order aberration $(:)\ \alpha\beta$. Outside the median plane three extra terms contribute: the sagittal second order angular aberration $(:)\ \alpha_z^2$; the image curvature $(:)\ \delta^2$; and the agammatism $(:)\ \alpha_z\,\delta$. Here α_z is the axial aperture angle, and δ is the distance of the object point from the median plane.

What aberrations can occur, as well as their influence on the shape and sharpness of the image, may be deduced from symmetry considerations (BOERBOOM [2]). The six terms mentioned above are those related to y-focusing with an infinitely narrow object slit. With object slits of finite width two extra terms occur, causing distorsion, and rotation of the image plane. Distorsion results in a slight displacement of an otherwise sharp image, and in a small slope of the "flat" top of an ideal peak. Rotation of the image plane could be compensated for by rotating the image slit around its z-axis. In actual cases, however, the width of the image slit is always so small that the influence of the latter two terms is entirely negligible.

1. Coordinate system

In the following calculations, it is again assumed that the field can be approximated by a ψ-independent field within the field boundaries, where it falls off abruptly to zero. For the present, only the case is treated where the field boundaries are plane and normal to the main path at the points where it enters and leaves the field.

The coordinate system is identical to that used in the previous article [1]. In the field free object and image space, the rectilinear trajectories are expressed in the cartesian coordinates x_1, y_1, z_1, and x_2, y_2, z_2, respectively. In the magnetic field region the radius of the main path is r_m, and the curved ion trajectories are expressed in the dimensionless coordinates: $u=(r-r_m)/r_m$; $v=z/r_m$; $w=\psi$, see Fig. 1 *. At the boundaries the tangents to the curved paths in the field region are supposed to coincide with the straight paths in the object and image space.

2. First and second approximation of the ion trajectories

The first order approximation has been derived in the previous article [1]. The expressions [14] ** and [15] remain equally valid when the restriction to the median plane is dropped. Analogous to [16] we now have the simultaneous differential equations defining the second order approximation:

$$u''-2\,F_{20}\,u-F_{10}=u\,u''+\tfrac{1}{2}(u'^2-v'^2)+3\,F_{30}\,u^2+F_{12}\,v^2; \tag{1}$$

$$v''-2\,F_{02}\,v=u\,v''+u'\,v'+2\,F_{12}\,u\,v. \tag{2}$$

(2) gives the second order approximation related to focusing in the v direction (or z direction). This will not concern us here for reasons explained above. Thus we need only solve (1), which can be accomplished by the method of variation of parameters if we write the right hand member of (1) as a function of w, say $F(w)$. To achieve this, we substitute the first order approximation [14], [15], into the right hand member of (1), analogous to [17]. Evaluation of $F(w)$ then results in:

$$\begin{aligned}F(w)=&\,C_1\cos^2 k_1 w+C_2\sin k_1 w\cos k_1 w+C_3\sin^2 k_1 w\\&+C_4\cos k_1 w+C_5\sin k_1 w+C_6\\&+C_7\cos^2 k_2 w+C_8\sin k_2 w\cos k_2 w\\&+C_9\sin^2 k_2 w,\end{aligned} \tag{3}$$

where C_1, C_2, C_3, C_4, C_5, and C_6, are given by [19], and:

$$\begin{aligned}C_7&=F_{12}\,v_0^2-\tfrac{1}{2}\,\alpha_z^2,\\C_8&=2\,F_{12}\,k_2^{-1}\,v_0\,\alpha_z+k_2\,v_0\,\alpha_z,\\C_9&=k_2^{-2}\,F_{12}\,\alpha_z^2-\tfrac{1}{2}\,k_2^2\,v_0^2.\end{aligned} \tag{4}$$

[2] A. J. H. BOERBOOM, Thesis, Leyden 1957; Appl. Sci. Res. B 7, 52 [1958].
* Figs. 1 and 2 are presented in the next paper.
** Numbers in square brackets [ ] refer to expressions in the previous paper [1].

(For reasons of conformation with the notation of other authors, we now designate the boundary condition $(\mathrm{d}v/\mathrm{d}w)_{w=0} = \alpha_z$.)

Now (1) may be solved by the general formula [18]. Straightforward integration leads to the second order approximation:

$$u = {}^{(2)}u(w) = H_1\, u_0 + H_2\, \alpha + H_3 + H_{11}\, u_0^2 + H_{12}\, u_0\, \alpha + H_{22}\, \alpha^2 + H_{44}\, v_0^2 + H_{45}\, v_0\, \alpha_z + H_{55}\, \alpha_z^2 . \tag{5}$$

H_1, H_2, H_3, H_{11}, H_{12}, and H_{22} are given by [20], and:

$$\begin{aligned} H_{44} &= \tfrac{1}{2} F_{12}\, k_1^{-2} (k_1^2 - 4\, k_2^2)^{-1} \{k_1^2 \cos 2\, k_2\, w - 2\,(k_1^2 - 2\, k_2^2) \cos k_1\, w + k_1^2 - 4\, k_2^2\} \\ &\quad + \tfrac{1}{4} k_2^2\, k_1^{-2} (k_1^2 - 4\, k_2^2)^{-1} \{k_1^2 \cos 2\, k_2\, w - 4\, k_2^2 \cos k_1\, w - k_1^2 + 4\, k_2^2\}; \\ H_{45} &= \tfrac{1}{2} k_1^{-1}\, k_2^{-1} (2\, F_{12} + k_2^2)\, (k_1^2 - 4\, k_2^2)^{-1} \{k_1 \sin 2\, k_2\, w - 2\, k_2 \sin k_1\, w\}; \\ H_{55} &= -\tfrac{1}{2} F_{12}\, k_1^{-2}\, k_2^{-2} (k_1^2 - 4\, k_2^2)^{-1} \{k_1^2 \cos 2\, k_2\, w - 4\, k_2^2 \cos k_1\, w - k_1^2 - 4\, k_2^2\} - \tfrac{1}{4} k_1^{-2} (k_1^2 - 4\, k_2^2)^{-1} \\ &\quad \{k_1^2 \cos 2\, k_2\, w - 2\,(k_1^2 - 2\, k_2^2) \cos k_1\, w + k_1^2 - 4\, k_2^2\} . \end{aligned} \tag{6}$$

The coefficients in (5) are correlated to the magnetic field shape by [8], [9], and [32]. After substitution of these relations, the resulting expression should be expanded in a TAYLOR series in the relative momentum spread β as defined by [34] or [35], where terms up to the second order in u_0, α, v_0, α_z, and β, should be retained. Thus the second order approximation of the ion trajectories reads:

$$\begin{aligned} u = {}^{(2)}u(w) &= D_1\, u_0 + D_2\, \alpha + D_3\, \beta + D_{11}\, u_0^2 + D_{12}\, u_0\, \alpha + D_{22}\, \alpha^2 + D_{13}\, u_0\, \beta + D_{23}\, \alpha\, \beta + D_{33}\, \beta^2 + D_{44}\, v_0^2 \\ &\quad + D_{45}\, v_0\, \alpha_z + D_{55}\, \alpha_z^2 . \end{aligned} \tag{7}$$

With the abbreviations: $w^* = (1-n)^{1/2}\, w$, and $w^\dagger = n^{1/2}\, w$ the expressions D_j are given by [37] and:

$$\begin{aligned} D_{44} &= \frac{1}{4} (1 - 5\, n)^{-1} \{\langle 2\, n - X(1-n) \rangle \cos 2\, w^\dagger - 2\,(n - X + 3\, n\, X) \cos w^* - X(1 - 5\, n)\}, \\ D_{45} &= \frac{1}{2} n^{-1/2} (1-n)^{-1/2} (1 - 5\, n)^{-1} \langle 2\, n - X(1-n) \rangle \{(1-n)^{1/2} \sin 2\, w^\dagger - 2\, n^{1/2} \sin w^*\}, \\ D_{55} &= -\frac{1}{4} n^{-1} (1 - 5\, n)^{-1} \{\langle 2\, n - X(1-n) \rangle \cos 2\, w^\dagger - 2\,(n - 2\, n\, X) \cos w^* + X(1 - 5\, n)\} . \end{aligned} \tag{8}$$

From Fig. 2 * we read the relations: (omitting terms of third and higher order)

$$\left.\begin{aligned} u_0 &= (l_m'/r_m)\, \alpha_m , \\ \alpha &= \alpha_m + (l_m'/r_m)\, \alpha_m^2, \\ v_0 &= (l_m'/r_m)\, \alpha_{zm} + \delta/r_m , \\ \alpha_z &= \alpha_{zm} \end{aligned}\right\} \tag{9}$$

whilst:

$$\left.\begin{aligned} y_2 &= r_m\, u(W) + (\mathrm{d}y_2/\mathrm{d}x_2)_{x_2=0} \cdot x_2 , \\ z_2 &= r_m\, v(W) + (\mathrm{d}z_2/\mathrm{d}x_2)_{x_2=0} \cdot x_2 , \\ (\mathrm{d}y_2/\mathrm{d}x_2)_{x_2=0} &= u'(W) \cdot (1 - u(W)), \\ (\mathrm{d}z_2/\mathrm{d}x_2)_{x_2=0} &= v'(W) \cdot (1 - u(W)), \end{aligned}\right\} \tag{10}$$

where W is the sector angle.

Substituting the expressions (9) and (10) into (7), we find the equation of the ion trajectory in the image space (y_2 in second order approximation, z_2 in first order approximation):

$$\begin{aligned} y_2 = r_m\, &\{M_1\, \alpha_m + M_2\, \beta + M_{11}\, \alpha_m^2 + M_{12}\, \alpha_m\, \beta \\ &+ M_{22}\, \beta^2 + M_{33}\, \alpha_{zm}^2 \\ &+ M_{34} (\delta/r_m)\, \alpha_{zm} + M_{44} (\delta/r_m)^2\} \\ &+ x_2 \{N_1\, \alpha_m + N_2\, \beta + N_{11}\, \alpha_m^2 + N_{12}\, \alpha_m\, \beta + N_{22}\, \beta^2 \\ &+ N_{33}\, \alpha_{zm}^2 + N_{34} (\delta/r_m)\, \alpha_{zm} + N_{44} (\delta/r_m)^2\} . \end{aligned} \tag{11}$$

$$\begin{aligned} z_2 = r_m\, &\{\Sigma_3\, \alpha_{zm} + \Sigma_4 (\delta/r_m)\} \\ &+ x_2 \{T_3\, \alpha_{zm} + T_4 (\delta/r_m)\} . \end{aligned} \tag{12}$$

The coefficients M_i, N_i, Σ_i, T_i, are given by [43], [44], and:

$$\left.\begin{aligned} M_{33} &= \mu_{33a} + \mu_{33b} (l_m'/r_m) + \mu_{33c} (l_m'/r_m)^2, \\ M_{34} &= \mu_{34a} + \mu_{34b} (l_m'/r_m), \\ M_{44} &= \mu_{44a}; \end{aligned}\right\} \tag{13}$$

$$\left.\begin{aligned} N_{33} &= \nu_{33a} + \nu_{33b} (l_m'/r_m) + \nu_{33c} (l_m'/r_m)^2, \\ N_{34} &= \nu_{34a} + \nu_{34b} (l_m'/r_m), \\ N_{44} &= \nu_{44a}; \end{aligned}\right\} \tag{14}$$

$$\Sigma_3 = \sigma_{3a} + \sigma_{3b} (l_m'/r_m), \qquad \Sigma_4 = \sigma_{4a}; \tag{15}$$

$$T_3 = \tau_{3a} + \tau_{3b} (l_m'/r_m), \qquad T_4 = \tau_{4a} . \tag{16}$$

The expressions [43] – [44], (11) – (16), are valid for any arrangement as in Fig. 2. For the particular field shape specified by [32] and [33], the coefficients μ_i, ν_i, σ_i, and τ_i are given by [45], [46], and:

$$\mu_{33a} = -\tfrac{1}{4}n^{-1}(1-5\,n)^{-1}\{\langle 2\,n - X(1-n)\rangle \cos 2\,W^\dagger - 2\,n(1-2\,X)\cos W^* + X(1-5\,n)\},$$
$$\mu_{33b} = \mu_{34a} = \tfrac{1}{2}(1-5\,n)^{-1}\,n^{-1/2}(1-n)^{-1/2}\langle 2\,n - X(1-n)\rangle\{(1-n)^{1/2}\sin 2\,W^\dagger - 2\,n^{1/2}\sin W^*\}, \tag{17}$$
$$\mu_{33c} = \tfrac{1}{2}\mu_{34b} = \mu_{44a} = \tfrac{1}{4}(1-5\,n)^{-1}\{\langle 2\,n - X(1-n)\rangle \cos 2\,W^\dagger - 2\langle n - X(1-3\,n)\rangle \cos W^* - X(1-5\,n)\};$$

$$\nu_{33a} = \tfrac{1}{2}n^{-1}(1-5\,n)^{-1}\{n^{1/2}\langle 2\,n - X(1-n)\rangle \sin 2\,W^\dagger + (1-n)^{1/2}\,n(2\,X-1)\sin W^*\},$$
$$\nu_{33b} = \nu_{34a} = (1-5\,n)^{-1}\langle 2\,n - X(1-n)\rangle(\cos 2\,W^\dagger - \cos W^*),$$
$$\nu_{33c} = \tfrac{1}{2}\nu_{34b} = \nu_{44a} = \tfrac{1}{2}(1-5\,n)^{-1}\{-\langle 2\,n - X(1-n)\rangle\,n^{1/2}\sin 2\,W^\dagger + \langle n - X(1-3\,n)\rangle(1-n)^{1/2}\sin W^*\}; \tag{18}$$

$$\sigma_{3a} = n^{-1/2}\sin W^\dagger, \qquad \sigma_{3b} = \sigma_{4a} = \tau_{3a} = \cos W^\dagger, \qquad \tau_{3b} = \tau_{4a} = -n^{1/2}\sin W^\dagger. \tag{19}$$

In [45] – [46], (16) – (19), the abbreviations:

$$W^* = (1-n)^{1/2}\,W, \quad \text{and} \quad W^\dagger = n^{1/2}\,W$$

have been used.

3. The second order aberrations outside the median plane

In the previous article[1] it was shown, that first order direction focusing occurs at the image distance $l_m'' = r_m(-M_1/N_1)$. We substitute therefore $x_2 = r_m(-M_1/N_1)$ in (11) and (12), and find for the image broadening due to the sagittal second order angular aberration:

$$A_{33}\,\alpha_{zm}^2 = r_m\{M_{33} - (M_1/N_1)\,N_{33}\}\,\alpha_{zm}^2; \tag{20}$$

the image curvature broadens the image by the amount:

$$A_{44}(\delta/r_m)^2 = r_m\{M_{44} - (M_1/N_1)\,N_{44}\}(\delta/r_m)^2; \tag{21}$$

whilst the agammatism has the effect:

$$A_{34}\,\alpha_{zm}(\delta/r_m) = r_m\{M_{34} - (M_1/N_1)\,N_{34}\}\,\alpha_{zm}(\delta/r_m). \tag{22}$$

If all ions travel parallel to the median plane ($\alpha_{zm} = 0$), (12) reduces to:

$$z_2 = \{\Sigma_4 - (M_1/N_1)\,T_4\}\,\delta. \tag{23}$$

Eliminating δ from (21) and (23), we find the radius of curvature of the image:

$$R_{im} = r_m \cdot \tfrac{1}{2}\,\frac{\{\Sigma_4 - (M_1/N_1)\,T_4\}^2}{M_{44} - (M_1/N_1)\,N_{44}}. \tag{24}$$

A positive value of R_{im} means that the centre of curvature has a positive y_2-coordinate.

So far the influence of fringing fields was neglected. It was demonstrated by BERRY[3] that for homogeneous magnetic sector fields with plane field boundaries that are normal to the main path, the fringing fields cause image curvature with a radius of curvature that is independent of the shape of the fringing fields or the sector angle, and which is in our notation given by:

$$R_{fr} = r_m\,\frac{N_1}{1-N_1}, \tag{25}$$

where use is made of [57]. (See also SEPTIER[4].) The influence of the fringing fields on the α_{zm}^2- and $\alpha_{zm}(\delta/r_m)$-aberrations was also calculated by BERRY[3], who found that their influence could be reduced by limiting the extension of the fringing fields by shields. One of the assumptions made in the derivations of (25) is no longer valid for inhomogeneous magnetic sector fields: the stray field outside the median plane has a non-negligible y-component. However, it may be expected that (25) is still essentially correct; the resulting radius of curvature is then given by:

$$R_{total} = \frac{R_{im}\,R_{fr}}{R_{im} + R_{fr}}. \tag{26}$$

4. Numerical example

Evaluation of (20), (21), (22), and (24) for the same case as treated in the previous paper[1] (i. e. $W = \pi$; $n = 0.91$; $X = 0.22131$; which gives radial second order angular focusing with object and image distances equal to $l_m' = l_m'' = 6.542\,r_m$), we find:

$$A_{33} = -32.639\,r_m; \qquad A_{34} = -10.390\,r_m;$$
$$A_{44} = -0.810\,r_m.$$

From (24) the radius of the image curvature due to the inhomogeneous magnetic sector field equals: $R_{im} = -2.203\,r_m$. (25) gives the image curvature due to the fringing fields with a radius

$$R_{fr} = -0.500\,r_m$$

and thus the radius of the total image curvature equals $R_{total} = -0.408\,r_m$. The negative sign of the

[3] C. E. BERRY, Rev. Sci. Instruments **27**, 849 [1956].
[4] A. SEPTIER, Sur le champ de fuite des déflecteurs magnétiques, etc. CERN 59–1 (Dec. 1958).

R_{total} indicates that the centre of curvature has a negative y_2-coordinate.

The results of this work were obtained independently in Munich and Amsterdam.

The authors wish to thank Prof. Dr. H. EWALD and Prof. Dr. J. KISTEMAKER respectively for their stimulating interest.

The work made in Munich was made possible by financial support of the Bundesministerium für Atomkernenergie und Wasserwirtschaft in Bad Godesberg. The work made in Amsterdam is part of the program of research of the Stichting voor Fundamenteel Onderzoek der Materie, and was made possible by financial support of the Nederlandse Organisatie voor Zuiver Wetenschappelijk Onderzoek.

Calculation of the Ion Optical Properties of Inhomogeneous Magnetic Sector Fields
Part 3: Oblique Incidence and Exit at Curved Boundaries

By H. A. TASMAN and A. J. H. BOERBOOM

F.O.M.-Laboratorium voor Massaspectrografie, Amsterdam, Holland,

and H. WACHSMUTH

Physikalisches Institut der Technischen Hochschule, München

(Z. Naturforschg. 14 a, 822—827 [1959]; eingegangen am 14. Juni 1959)

In previous papers [1, 2] we presented the radial second order imaging properties of inhomogeneous magnetic sector fields with normal incidence and exit at plane boundaries. These fields may provide very high mass resolving power and mass dispersion without increase in radius or decrease of slit widths. In the present paper the calculations are extended to include the effect of oblique incidence and exit at curved boundaries. The influence of the fringing fields on axial focusing when the boundaries are oblique, is accounted for. It is shown that the second order angular aberration may be eliminated by appropriate curvature of the boundaries.

In previous papers (TASMAN and BOERBOOM [1]; WACHSMUTH, BOERBOOM and TASMAN [2]) we calculated the imaging properties of inhomogeneous magnetic sector fields with normal incidence and exit of the main path at plane boundaries. The median plane was supposed to be a plane of symmetry for the magnetic vector potential.

The present paper deals with the most general case if the symmetry with respect to the median plane is retained, i. e. that of curved oblique boundaries. The sector field approximation is retained, i. e. the field strength is supposed to be independent of the path coordinate within the field boundaries where it falls off to zero abruptly. The field boundaries are assumed to consist of lines normal to the median plane. The influence of the fringing fields on axial focusing when the boundaries are oblique, is accounted for.

The coordinate system is identical to that used in the previous paper [2] (Fig. 1). Some of the relevant parameters are shown in Fig. 2. The shape of the boundaries is defined by the projection on the median plane (Fig. 3). The obliqueness at the entrance and exit of the main path is defined by the

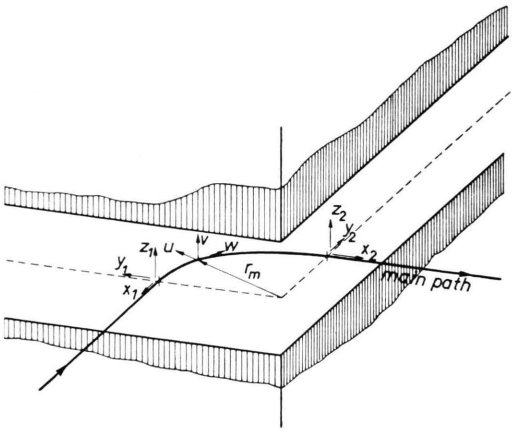

Fig. 1.

angles ε' and ε''. These quantities are positive as shown in Fig. 3. The radii of curvature of the entrance and exit boundaries are R' and R'', which quantities are chosen to be positive if the corresponding boundary is convex towards field-free space. In Fig. 3, both R' and R'' are positive.

[1] H. A. TASMAN and A. J. H. BOERBOOM, Z. Naturforschg. **14 a**, 121 [1959].

[2] H. WACHSMUTH, A. J. H. BOERBOOM and H. A. TASMAN, Z. Naturforschg. **14 a**, 818 [1959].